

1 **The effects of introgression across thousands of quantitative traits revealed by gene**
2 **expression in wild tomatoes**

3

4 Mark S. Hibbins* and Matthew W. Hahn*,†

5

6 *Department of Biology and †Department of Computer Science, Indiana University,
7 Bloomington, IN 47405

8

9

10

11

12

13

14

15

16

17

18

19

20

21

22

23

24

25

26

27

28

29

30 **Abstract**

31 It is now understood that introgression can serve as powerful evolutionary force, providing
32 genetic variation that can shape the course of trait evolution. Introgression also induces a shared
33 evolutionary history that is not captured by the species phylogeny, potentially complicating
34 evolutionary analyses that use a species tree. Such analyses are often carried out on gene
35 expression data across species, where the measurement of thousands of trait values allows for
36 powerful inferences while controlling for shared phylogeny. Here, we present a Brownian
37 motion model for quantitative trait evolution under the multispecies network coalescent
38 framework, demonstrating that introgression can generate apparently convergent patterns of
39 evolution when averaged across thousands of quantitative traits. We test our theoretical
40 predictions using whole-transcriptome expression data from ovules in the wild tomato genus
41 *Solanum*. Examining two sub-clades that both have evidence for post-speciation introgression,
42 but that differ substantially in its magnitude, we find patterns of evolution that are consistent
43 with histories of introgression in both the sign and magnitude of ovule gene expression.
44 Additionally, in the sub-clade with a higher rate of introgression, we observe a correlation
45 between local gene tree topology and expression similarity, implicating a role for introgressed
46 *cis*-regulatory variation in generating these broad-scale patterns. Our results reveal a general role
47 for introgression in shaping patterns of variation across many thousands of quantitative traits,
48 and provide a framework for testing for these effects using simple model-informed predictions.

49

50

51 **Introduction**

52 Introgression—the historical hybridization and subsequent backcrossing of previously isolated
53 lineages—has come to the forefront of phylogenomics with the availability of genome
54 sequencing (reviewed in Mallet et al 2016, Taylor and Larson 2019). Introgression has been
55 recognized as a powerful and frequent source of adaptive variation, with many charismatic
56 examples including wing pattern mimicry in butterflies (Pardo-Diaz et al. 2012, Zhang et al.
57 2016), coat color in snowshoe hares (Jones et al. 2018), herbivore resistance in sunflowers
58 (Whitney et al. 2006), high-altitude adaptation in humans (Huerta-Sánchez et al. 2014), and fruit
59 color in wild tomatoes (Gibson et al. 2021). Introgressed alleles do not have to underlie discrete
60 traits to influence the course of evolution: alleles that contribute to quantitative trait variation can
61 also lead to more similarity than expected between the introgressing lineages (Bastide et al.
62 2018).

63 Empirically investigating the effects of introgressed ancestry on quantitative trait evolution
64 remains a challenge, despite recent theoretical and methodological advances (Bastide et al. 2018,
65 Hibbins et al. 2020, Wang et al. 2020). This is because many processes besides introgression can
66 shape the distribution of any particular character, including incomplete lineage sorting and
67 convergence. It is therefore necessary to sample a large number of traits in order to demonstrate
68 a genome-wide effect of introgression. Gene expression is commonly used in comparative
69 analyses between species (e.g. Rifkin et al. 2003, Brawand et al. 2011, Davidson et al. 2012),
70 allowing for the study of thousands of quantitative traits in a phylogenetic framework.
71 Introgressed variants acting on gene expression either in *cis* or in *trans* may affect the evolution
72 of gene expression across the genome. This could have potentially deleterious effects on fitness,
73 which would be consistent with previous evidence for widespread selection against introgressed
74 alleles (Brandvain et al. 2014, Sankararaman et al. 2014, Schumer et al. 2018, Martin et al.
75 2019).

76 Incomplete lineage sorting (ILS) and introgression both introduce shared history that could
77 influence the evolution of quantitative traits, though neither of these processes are captured by a
78 standard species phylogeny. Therefore, to paint a complete picture of trait variation among
79 species, it is necessary to include these sources of topological discordance in order to avoid
80 errors inherent to methods that typically only consider the species topology (Hahn and Nakhleh
81 2016). Mendes et al. (2018) showed that when gene tree discordance is unaccounted for,
82 standard comparative approaches will return inflated evolutionary rate estimates and will
83 underestimate phylogenetic signal. Despite these challenges, no approach has included all
84 sources of gene tree discordance into a single framework for quantitative trait evolution. Some
85 methods have extended the classic Brownian motion model for quantitative trait evolution to
86 include shared histories due to ILS alone (Mendes et al. 2018), while other work has applied the
87 Brownian motion model to a phylogenetic network with introgression but no ILS (Bastide et al.
88 2018). A method including both sources of discordance would provide a complete picture of the
89 most common causes of shared evolutionary history and their effects on quantitative traits. This
90 would in turn allow for more accurate inferences of key evolutionary parameters, such as the trait
91 evolutionary rate.

92 To address the effects of historical introgression on quantitative traits, we first develop a
 93 Brownian motion model of trait evolution that includes both ILS and introgression, showing the
 94 expected effects of introgression on the similarity in quantitative traits across species. This model
 95 leads directly to predictions about patterns of trait-sharing on a three-taxon tree, which we test by
 96 leveraging whole-transcriptome gene expression data (Moyle et al. 2021) from the wild tomato
 97 clade in the genus *Solanum*. This clade includes 13 species that have radiated within the last 2.5
 98 million years, and contains high rates of gene tree discordance due to both ILS and introgression
 99 (Pease et al. 2016, Hamlin et al. 2020). Using ovule expression data from two independent
 100 species triplets with different levels of introgression, we find that transcriptome-wide patterns of
 101 variation in both triplets are consistent with histories of introgression, with quantitatively
 102 stronger signals in the sub-clade with greater introgression. Our analyses demonstrate that
 103 introgression can have measurable effects across the genome, on thousands of quantitative traits.

104 **Results**

105 **Brownian motion on a species tree**

106 To accurately model trait variation among species, we require an understanding of the
 107 evolutionary history that relates those species, and a model for how traits are expected to evolve
 108 given that history. We present results using Brownian motion, a statistical model that is
 109 commonly applied to quantitative traits. The evolutionary history relating species has classically
 110 been provided by a species phylogeny. Under Brownian motion, the character states on the tips
 111 of this phylogeny follow a multivariate normal distribution, with the variance and covariances of
 112 this distribution provided by the branch lengths of the phylogeny (Felsenstein 1973).

113 Consider a phylogeny of three species with the topology ((A,B),C) (Figure 1). In units of $2N$
 114 generations, species A and B split at time t_1 , and C split from the ancestor of A and B at time t_2 .
 115 The expected phylogenetic variances and covariances for three species can be expressed in a 3×3
 116 matrix, which we denote \mathbf{T} :

$$117 \quad \mathbf{T} = \begin{bmatrix} \text{Var}(A) & \text{Cov}(AB) & \text{Cov}(AC) \\ \text{Cov}(BA) & \text{Var}(B) & \text{Cov}(BC) \\ \text{Cov}(CA) & \text{Cov}(CB) & \text{Var}(C) \end{bmatrix} \quad [1]$$

118 This matrix is multiplied by the evolutionary rate parameter of the Brownian motion model, σ^2 ,
 119 to obtain trait variances and covariances. When only the species phylogeny is considered (i.e.
 120 there is no ILS or introgression), the trait variances (the diagonal elements of \mathbf{T}) are determined
 121 by the total time along which evolution can occur for each lineage, so $\text{Var}(A) = \text{Var}(B) = \text{Var}(C)$
 122 $= t_2$. The covariances are determined by the length of shared internal branches. In the species
 123 tree, only species A and B share an internal branch, so:

$$124 \quad \text{Cov}(AB \mid \text{no ILS or introgression}) = \sigma^2(t_2 - t_1) \quad [2]$$

125 Where σ^2 corresponds to the trait evolutionary rate per unit time, and $\text{Cov}(AB) = \text{Cov}(BA)$.

126 In the absence of other processes, the species pairs BC and AC have zero covariance. However,
 127 trees inferred at individual loci can disagree with the species phylogeny, in which case these

128 species pairs could have shared internal branches, and therefore non-zero covariances. This
 129 widespread phenomenon is known as gene tree discordance (e.g. Pollard et al. 2006, White et al.
 130 2009, Hobolth et al. 2011, Fontaine et al. 2015, Pease et al. 2016, Wu et al. 2018, Vanderpool et
 131 al. 2020, Hime et al. 2021) and has multiple biological causes (Degnan and Rosenberg 2009).
 132 Gene trees with the topologies ((B,C),A) or ((A,C),B) contain internal branches shared by
 133 species B+C and A+C, respectively (Figure 1). This results in non-zero covariance terms
 134 between these two species pairs in \mathbf{T} , covariance that cannot arise from evolution solely on the
 135 species phylogeny. The consequence of this discordance is that some traits may be closer in
 136 value between species that are not closely related in the species tree. We must therefore include
 137 discordance in our model to appropriately capture this trait covariance.

138 **Modelling the effects of only incomplete lineage sorting on quantitative trait variances and**
 139 **covariances**

140 One of the most common causes of gene tree discordance is incomplete lineage sorting, which
 141 occurs when ancestral lineages persist through successive speciation events (Hudson 1983,
 142 Pamilo and Nei 1988). For a rooted triplet, there are four possible gene trees in the presence of
 143 ILS: one concordant tree that occurs by lineage sorting with probability $1 - e^{-(t_2 - t_1)}$, and
 144 three trees produced by ILS, each with probability $\frac{1}{3} e^{-(t_2 - t_1)}$. One of the three ILS trees is
 145 concordant, while the other two are discordant. These probabilities are the basis for the
 146 multispecies coalescent model. To obtain the expected trait variances and covariances in \mathbf{T} ,
 147 Mendes et al. (2018) weight the expected gene tree heights and internal branch lengths,
 148 respectively, by their expected frequencies under the multispecies coalescent model. We present
 149 those results here with a slightly different formulation for consistency with the new results
 150 presented below. For the covariance between A and B, we have:

$$\begin{aligned}
 &151 \quad \text{Cov}(AB \mid \text{no introgression}) \\
 &152 \quad = \sigma^2 \left[(1 - e^{-(t_2 - t_1)}) \left(\frac{e^{t_2}(t_2 - t_1)}{e^{t_2} - e^{t_1}} \right) + \left(\frac{1}{3} e^{-(t_2 - t_1)} \right) \right] \quad [3]
 \end{aligned}$$

153 In equation 3, σ^2 corresponds to the trait evolutionary rate per $2N$ generations, which is the scale
 154 over which time is measured in the multispecies coalescent model. Inside the square brackets, the
 155 first term is the probability of the gene tree produced by lineage sorting, multiplied by that tree's
 156 expected internal branch length in units of $2N$ generations. The second term is the probability of
 157 the concordant tree produced by ILS, which has an expected internal branch length of 1 in units
 158 of $2N$ generations.

159 Species pairs BC and AC can only have covariance from discordant trees produced by ILS,
 160 which gives:

$$\begin{aligned}
 &161 \quad \text{Cov}(BC \mid \text{no introgression}) = \text{Cov}(AC \mid \text{no introgression}) \\
 &162 \quad = \sigma^2 \left(\frac{1}{3} e^{-(t_2 - t_1)} \right) \quad [4]
 \end{aligned}$$

163 Again, in these trees the internal branches are of length 1 in units of $2N$ generations, and so are
 164 not shown explicitly.

165 For the expected trait variances, all three species share the same expected variance, which is the
 166 total height of all the gene trees weighted by their probabilities. These are:

$$167 \quad \text{Var}(A \mid \text{no introgression}) = \text{Var}(B \mid \text{no introgression}) = \text{Var}(C \mid \text{no introgression}) = \\
 168 \quad \sigma^2 \left[(1 - e^{-(t_2-t_1)})(t_2 + 1) + (e^{-(t_2-t_1)})(t_2 + 1 + 1/3) \right] \quad [5]$$

169 Where the first term in the square brackets is the contribution from the lineage sorting tree, and
 170 the second term is the contribution from the three ILS trees.

171 **Modelling the effects of introgression and ILS on quantitative trait variances and** 172 **covariances**

173 Now, we extend these expressions for species variances and covariances to include both ILS and
 174 introgression. We envision an instantaneous introgression event between species B and C (Figure
 175 1), which occurs at time t_m . This event can be in either direction, with the probabilities of a locus
 176 following a history of $C \rightarrow B$ introgression or $B \rightarrow C$ introgression represented using δ_2 or δ_3 ,
 177 respectively. To capture the processes of ILS and introgression simultaneously, we imagine that
 178 each possible history at an individual locus can be represented by a “parent tree” within which
 179 lineage sorting or ILS occurs according to the multispecies coalescent process (Meng and
 180 Kubatko 2009, Liu et al. 2014, Hibbins and Hahn 2019, Hibbins et al. 2020). This is sometimes
 181 referred to as the multispecies network coalescent (Wen et al. 2016, Degnan 2018). For our
 182 model, we consider three parent trees (see Supplementary Figure 2): one with no introgression,
 183 which occurs with probability $1 - (\delta_2 + \delta_3)$, and two parent trees for the two possible directions
 184 of introgression, which occur with probabilities of either δ_2 or δ_3 (these probabilities represent
 185 the “rate” of introgression in our model). Each of these three parent trees can generate four
 186 possible gene trees with three possible topologies (Figure 1, arrow 1), which vary in the
 187 frequency of topologies and expected branch lengths depending on each parent tree's parameters
 188 (as in the model of ILS-only described in the previous section).

189 To obtain expressions for the expected variances and covariances under this model, we must sum
 190 the contributions of all gene trees within each parent tree, and then sum the contribution of each
 191 parent tree (Figure 1, arrow 2). For the covariance between A and B, this gives:

$$192 \quad \text{Cov}(AB \mid \text{ILS and introgression}) \\
 193 \quad = \sigma^2 \left[(1 - (\delta_2 + \delta_3)) \left[(1 - e^{-(t_2-t_1)}) \left(\frac{e^{t_2}(t_2 - t_1)}{e^{t_2} - e^{t_1}} \right) + \left(\frac{1}{3} e^{-(t_2-t_1)} \right) \right] \right. \\
 194 \quad \left. + \delta_2 \left(\frac{1}{3} e^{-(t_2-t_m)} \right) + \delta_3 \left(\frac{1}{3} e^{-(t_1-t_m)} \right) \right] \quad [6]$$

195 Note that the term inside the inner square brackets in equation 6 is the same as in equation 3, but
 196 is now weighted by the probability of a history with no introgression. In addition, there are two
 197 additional terms denoting the contributions of trees generated by ILS that follow a history of

198 introgression (because ILS occurs regardless of the history at a locus). For a complete derivation,
 199 including the expectations of each gene tree within each parent tree, see the Supplementary
 200 Materials and Methods.

201 For the covariance between B and C, we have:

$$\begin{aligned}
 & \text{Cov}(BC \mid \text{ILS and introgression}) \\
 &= \sigma^2 \left[(1 - (\delta_2 + \delta_3)) \left[\frac{1}{3} e^{-(t_2-t_1)} \right] \right. \\
 &+ \delta_2 \left[(1 - e^{-(t_2-t_m)}) \left(\frac{e^{t_2}(t_2 - t_m)}{e^{t_2} - e^{t_m}} \right) + \left(\frac{1}{3} e^{-(t_2-t_m)} \right) \right] \\
 &+ \left. \delta_3 \left[(-e^{-(t_1-t_m)}) \left(\frac{e^{t_1}(t_1 - t_m)}{e^{t_1} - e^{t_m}} \right) \left(\frac{1}{3} e^{-(t_1-t_m)} \right) \right] \right] \quad [7]
 \end{aligned}$$

206

207 Introgression occurs between B and C in our model, so B and C are sister in the parent trees that
 208 represent the two directions of introgression (see Supplementary Materials and Methods,
 209 Supplementary Figure 2). This means that these parent trees can each produce two gene trees
 210 with BC as sister species: one from lineage sorting and one from ILS. The contributions of these
 211 two gene trees in each parent tree are captured in the last two terms of equation 7. The first term
 212 corresponds to the contribution of ILS from the parent tree without introgression, i.e. equation 4.

213 Finally, for the covariance between A and C, we have

$$\begin{aligned}
 & \text{Cov}(AC \mid \text{ILS and introgression}) = \sigma^2 \left[(1 - (\delta_2 + \delta_3)) \left(\frac{1}{3} e^{-(t_2-t_1)} \right) + \right. \\
 & \left. \delta_2 \left(\frac{1}{3} e^{-(t_2-t_m)} \right) + \delta_3 \left(\frac{1}{3} e^{-(t_1-t_m)} \right) \right] \quad [8]
 \end{aligned}$$

216 Since gene trees where A and C are sister can only be produced by ILS in our model, equation 8
 217 is simply the sum of the gene trees with this topology produced by each of the three parent trees.

218 Lastly, we consider the expected trait variance with introgression. As with the covariances, we
 219 sum the total contribution of each gene tree within a parent tree, and then sum these
 220 contributions across each parent tree. All three share the same gene tree heights and therefore
 221 have the same expected variances. This gives:

$$\begin{aligned}
 & \text{Var}(A) = \text{Var}(B) = \text{Var}(C) \\
 &= \sigma^2 \left[(1 - (\delta_2 + \delta_3)) \left[(1 - e^{-(t_2-t_1)}) (t_2 + 1) + (e^{-(t_2-t_1)}) (t_2 + 1 + 1/3) \right] \right. \\
 &+ \delta_2 \left[(1 - e^{-(t_2-t_m)}) (t_2 + 1) + (e^{-(t_2-t_m)}) (t_2 + 1 + 1/3) \right] \\
 &+ \left. \delta_3 \left[(1 - e^{-(t_1-t_m)}) (t_1 + 1) + (e^{-(t_1-t_m)}) (t_1 + 1 + 1/3) \right] \right] \quad [9]
 \end{aligned}$$

226 The first term represents the contribution of the parent tree with no introgression, the same as in
 227 equation 5. The second two terms represent the contributions to the total variance from C → B
 228 and B → C introgression, respectively. When T is updated to include all these expectations, it

229 becomes possible to model character states under Brownian motion while accounting for both
230 ILS and introgression.

231 **Testing for the effect of introgression on quantitative traits**

232 To evaluate whether patterns of quantitative trait variation are consistent with a history of
233 introgression, we use a simple test statistic that employs the same logic as the D_3 test for
234 introgression (Hahn and Hibbins 2019; see also the f_3 statistic of Reich et al. 2009). Imagine that
235 species A, B, and C have values q_1 , q_2 , and q_3 for a hypothetical quantitative trait, respectively.
236 Given the species tree ((A,B),C), and assuming the Brownian motion model of trait evolution
237 described in the previous sections, the expected distance between trait values q_2 and q_3 should be
238 equal to the expected distance between q_1 and q_3 . This is because species C is equidistant to
239 species A and B in the phylogeny, and this tree determines quantitative trait variances and
240 covariances. The same relationship between distances is expected when considering the ILS-only
241 model, because of symmetries in expected gene tree frequencies and branch lengths, and
242 therefore in trait covariances (see equation 4).

243 However, introgression can introduce additional covariance between one pair of species,
244 resulting in that pair having more similar trait values than the other non-sister pair (see equations
245 7 and 8). This naturally leads to the following test statistic:

$$246 \quad Q_3 = \frac{|q_2 - q_3| - |q_1 - q_3|}{|q_2 - q_3| + |q_1 - q_3|} \quad [10]$$

247 The numerator of Q_3 takes the difference in trait distances between the two pairs of non-sister
248 species; when there is no introgression, this numerator—and therefore Q_3 —has an expected
249 value of 0. When a significant non-zero value of Q_3 is observed, the statistic is consistent with a
250 history of introgression. In addition, the sign of the statistic can tell us which species were
251 involved in introgression (but not the direction of introgression). For example, a negative Q_3
252 value would be consistent with introgression between species B and C, since that would result in
253 q_2 and q_3 having more similar values (and therefore a smaller distance between them). The
254 denominator of Q_3 is the sum of the two trait distances, which normalizes the statistic between 0
255 and 1, allowing it to be compared across traits with different mean values. We imagine that this
256 statistic will be applied to many individual quantitative traits, each providing a separate value of
257 Q_3 . The significance for a dataset consisting of many traits can then be evaluated either by
258 testing for a mean value of Q_3 significantly different from 0, or by using a sign test with the null
259 expectation that positive and negative Q_3 values should be equally frequent (see the analyses
260 below for more details).

261 To confirm the effects of introgression predicted by the model, and the ability of Q_3 to detect it,
262 we performed a power analysis. First, to illustrate the conceptual basis for Q_3 , we contrasted two
263 conditions: an ILS-only condition and an ILS + introgression condition (Figure 2). Both
264 scenarios use the three-taxon tree described in previous sections, simulating quantitative traits as
265 the sum of contributions of many genes (and therefore gene trees; see Methods). For 20,000
266 independent simulated traits we calculated the mean and standard error of the difference in trait
267 value at the tips of the tree between each pair of species (Figure 2). As predicted by our model,

268 the taxa involved in introgression had a higher covariance and more similar trait values than the
269 non-introgressing pair of taxa when averaging across the 20,000 traits (Figure 2).

270 Second, we performed a power analysis across 90 different parameter combinations: three values
271 each of the timing of introgression, the level of ILS, and the number of genes, and four values of
272 the rate of introgression. We simulated 100 datasets for each set of parameters and asked how
273 often Q_3 was significantly different from 0 in the direction predicted by introgression. We found
274 the most important parameter to be the rate of introgression: at a rate of 1% (i.e. 1% of the
275 genome has been introgressed), power was consistently low (1-6%) regardless of other
276 simulation parameters (Figure 3, Supplementary Figure 1). At higher rates of introgression,
277 power was increased when introgression was more recent relative to speciation, when the level
278 of ILS was lower, and when more genes (traits) were considered. When 5,000 genes were used,
279 power reached 67% under the best-case scenario (Supplementary Figure 1); this increased to
280 97% with 15,000 genes (Figure 3). Simulations under a no-introgression scenario yielded false
281 positive rates of less than 5% across all conditions (Supplementary Figure 2).

282 **Gene expression variation is consistent with inferred histories of introgression in *Solanum***

283 We used previously generated introgression and gene expression datasets from the wild tomato
284 clade, *Solanum* section *Lycopersicon*, to empirically evaluate the effects of introgression on
285 thousands of expression traits. This clade includes the domesticated tomato, *S. lycopersicum*, and
286 its 12 wild relatives, which have all originated in the last 2.5 million years. The first dataset is a
287 phylogenetic analysis of 29 accessions (i.e. populations) across these 13 tomato species and two
288 outgroups (Pease et al. 2016). This dataset includes an introgression analysis based on D -
289 statistics (Green et al. 2010, Durand et al. 2011) across all possible quartets, which provides a
290 comprehensive overview of patterns of introgression in the clade. The second dataset is
291 normalized quantitative expression of 14,556 genes expressed in ovules from six accessions
292 across five tomato species. This includes published data for five accessions across four species
293 (Moyle et al. 2021), while data from the other two species are previously unpublished.
294 Expression levels for each gene are represented as reads per kilobase of transcript, per million
295 mapped reads (RPKM). Samples were collected on the day of flower opening for 1-4 individuals
296 of each species grown in a common greenhouse (Moyle et al. 2021).

297 Combining these two datasets, we sought to identify triplets of species with both evidence of
298 introgression (from sequence data) and available gene expression data, so that we could apply
299 the Q_3 statistic. Additionally, we wanted these triplets to vary in the magnitude of introgression,
300 so that the magnitude of the effect of introgression on trait variation could be evaluated in
301 addition to the presence or absence of an effect. With these considerations in mind, we identified
302 two triplets. The first consists of the accessions LA3475 (*S. lycopersicum*), LA1589 (*S.*
303 *pimpinellifolium*), and LA0716 (*S. pennellii*), with LA3475 and LA1589 as sister taxa, and
304 evidence of introgression between LA1589 and LA0716 ($D = 0.057$, $P = 0.0015$, Pease et al.
305 2016) (Figure 4A). Using the D_p statistic (Hamlin et al. 2020) on site pattern counts from Pease
306 et al., we obtained a value of 0.0013, corresponding to a genomic rate of introgression of 0.13%.
307 We hereafter refer to this triplet as the “low” triplet because of the relatively low observed rate of
308 introgression. The other triplet consists of LA3778 (*S. pennellii*), LA1777 (*S. habrochaites*), and

309 *LA1316* (*S. chmielewskii*), with *LA3778* and *LA1777* as sister taxa, and significant introgression
310 between *LA1777* and *LA1316* ($D = 0.135$, $P = 2.34 \times 10^{-35}$, Pease et al. 2016) (Figure 4A). We
311 obtained a D_p value of 0.0744 for this triplet, corresponding to a rate of introgression of 7.44%;
312 this value is likely an underestimate, as D_p tends to underestimate the true value at higher rates of
313 introgression (Hamlin et al. 2020). As the rate of introgression is much higher for this triplet, we
314 refer to it as the “high” triplet.

315 We used expression values from 14,556 genes available in both the low and high triplets. For
316 each gene we calculated a separate value Q_3 , averaging across genes to obtain a mean value for
317 each triplet. We obtained transcriptome-wide mean Q_3 values of -0.012 and -0.019 for the low
318 and high triplet, respectively (Figure 4B). The values we observe are consistent with the histories
319 of introgression inferred from the sequence data in both sign and magnitude. Both triplets have
320 negative values, which is consistent with introgression between *S. pimpinellifolium* and *S.*
321 *pennellii* in the low triplet, and between *S. habrochaites* and *S. chmielewskii* in the high triplet
322 (see Figure 4A for the accessions assigned as q_1 , q_2 , and q_3 in each triplet). The Q_3 value is also
323 more negative in the high triplet, which is consistent with the higher level of introgression
324 inferred from sequence data.

325 The signal of introgression from quantitative traits was also statistically significant in both
326 triplets, using either method for assessing significance. Using a bootstrapping approach to ask
327 whether the mean values were different from 0 (see Methods), we obtained $P = 0.0012$ and $P <$
328 0.0001 for the low and high triplets, respectively (Figure 4B). We obtained similar results when
329 testing for a significant excess of either positive or negative Q_3 values (i.e. a sign test) at
330 individual genes using bootstrapping (Figure 4C; see Methods). For the low triplet, we observed
331 7432 negative and 7124 positive genes ($P = 0.0134$); for the high triplet, 7533 negative and 7020
332 positive genes ($P < 0.0001$). Again, the larger number of negative Q_3 values in the high triplet is
333 consistent with a higher amount of introgression.

334 **Gene-level analysis of expression data**

335 The expression level of genes can be affected by either *cis*-acting or *trans*-acting variants.
336 Because *cis*-acting variants are most often found near the gene they affect (Wray et al. 2003, Hill
337 et al 2020), we might expect these regulatory elements to share the same local gene tree topology
338 as the nearby genic protein-coding region; any signature of introgression would likely be
339 reflected in both regions. While recombination either before or after introgression will uncouple
340 the tree topology in the regulatory region from that in the coding region, we might expect to see
341 an association between patterns of similarity in expression levels and patterns of gene tree
342 discordance if *cis*-acting variants are common.

343 To test for such a relationship, we looked for an association between coding-region tree
344 topologies and expression similarity among species in both triplets. Using trees estimated from
345 each protein-coding gene (Pease et al. 2016), we identified 11,061 genes for which both the tree
346 topology and expression values from all species were available. For each gene, we obtained the
347 rooted tree topology for the relevant triplet and also determined which pair of species was most
348 similar in expression value. We assume that expression similarity reflects the local topology at

349 whichever locus has the largest effect on expression, such that the most similar pair of species
350 represents the sister species in this topology.

351 In the low triplet, we found no significant relationship ($P = 0.776$, χ^2 test of independence)
352 between protein-coding gene tree topology and expression similarity (Figure 5A). In the high
353 triplet, however, we did observe a significant relationship ($P = 0.019$, Figure 5B). For gene trees
354 with a topology consistent with introgression (where *S. habrochaites* and *S. chmielewskii* are
355 sister), there were significantly more genes where expression was also most similar between
356 these species than expected by chance (476 observed vs. 449 expected). In other words, we
357 found that gene expression similarity is correlated with the tree topology of protein-coding genes
358 in the high triplet, in a fashion consistent with *cis*-acting effects of introgressed variation on
359 expression.

360 **Discussion**

361 Phylogenetic comparative methods provide powerful tools for studying the origins of trait
362 variation among species. However, the rampant gene tree discordance uncovered in many
363 phylogenomic studies paints a more complicated picture of the shared history among species. To
364 date, most models of trait evolution employed by comparative methods have assumed that only
365 the species phylogeny contributes to trait covariance, and have ignored covariance due to
366 discordant gene trees. Our model builds on previous work (Mendes et al. 2018, Bastide et al.
367 2018) to incorporate both ILS and introgression into a single framework that captures the most
368 common causes of discordance and their effects on quantitative trait evolution. We show that
369 introgression leads to more discordance and stronger patterns of covariance in quantitative traits
370 among non-sister species than ILS alone, paralleling results for binary traits under the same
371 multispecies network coalescent framework (Hibbins et al. 2020).

372 Our model makes several assumptions and simplifications related to expected levels of genetic
373 covariance between species. First, we have modeled post-speciation introgression as a single
374 instantaneous pulse of exchange between one pair of non-sister species. Many other possible
375 introgression scenarios are possible, such as multiple pulses or continuous periods of gene flow.
376 Although each of these scenarios will increase the variance in gene tree topologies, we expect
377 that they will still leave a detectable signature on quantitative traits because they still lead to gene
378 tree asymmetries. In contrast, other gene flow scenarios—such as introgression between sister
379 taxa, or between both pairs of non-sister taxa in a triplet at equal rates—will not result in a
380 detectable signature of gene tree asymmetry. Second, we have assumed that the expected
381 frequencies and coalescence times of loci contributing to trait variation follow neutral
382 expectations. Through a local reduction in N_e , directional selection may reduce the rate of gene
383 tree discordance due to ILS, while increasing the rate of discordance due to introgression (Pease
384 and Hahn 2013, Munch et al. 2016, Martin et al. 2019). This increase in the rate of introgression
385 relative to ILS may allow for greater power to detect a signal of introgression in quantitative
386 traits, as we show in our power analysis. This implies that positive selection, especially on
387 introgressed variants (e.g. Setter et al. 2020), will make it more likely for quantitative traits to
388 covary between non-sister taxa.

389 We also make key assumptions about the model of trait evolution. Our model assumes that traits
390 evolve under a Brownian motion process, rather than alternative processes such as the Ornstein-
391 Uhlenbeck (OU) (Hansen 1997) or early-burst (Simpson 1944, Blomberg et al. 2003) models.
392 While it may be uncommon for traits to evolve according to an early-burst model (Harmon et al.
393 2010), many quantitative characters are likely to be constrained in some way, which can be
394 modelled by the OU process. For gene expression in particular, evidence suggests that over long
395 phylogenetic timescales the OU process is a better fit to the data (Bedford and Hartl 2009,
396 Catalán et al. 2019, Chen et al. 2019). However, multiple non-biological factors may favor the fit
397 of OU models over Brownian motion, including small amounts of error in measured quantitative
398 traits (Cooper et al. 2016). While we do not expect the model of trait evolution to affect
399 asymmetries between species in thousands of traits, future work incorporating additional models
400 of trait evolution, and their effect on trait covariances in particular, would be useful.

401 A key assumption of our statistical analysis is that each gene expression trait evolves
402 independently. However, many genes show correlated patterns of expression, either because of
403 locally shared *cis*-acting elements or because of *trans*-acting factors that affect the expression of
404 many genes across the genome (Wray et al. 2003, Hill et al 2020). If, for instance, such a *trans*-
405 acting factor is introgressed and affects many genes in a similar way, then treating each gene as
406 an independent observation would constitute pseudoreplication of measurements. However, there
407 are two pieces of evidence that suggest pseudoreplication is not a major problem in our analyses.
408 First, previous data from experimental introgression lines between *S. lycopersicum* and *S.*
409 *pennellii* are not consistent with a large role of introgressed loci on background gene expression:
410 Guerrero et al. (2016) found that each introgressed gene had downstream effects on the
411 expression of only 0.4 genes on average. Second, we find here that the number of genes where
412 expression is more similar between introgressing species is higher in the triplet with a higher rate
413 of introgression. This is again consistent with largely local effects of each introgressed locus on
414 gene expression. Based on these observations, we conclude that we likely have many thousands
415 of independent data points testing the relationship between introgression and expression
416 variation, even if the true correlation structure is unknown.

417 Our power analysis suggests that we should have had low power to detect an effect of
418 introgression in the low triplet, which has a rate of introgression of less than 1%. One
419 explanation **for the fact that we do detect an effect** that the introgressed variation in this triplet
420 affects the downstream regulation of a large set of correlated genes, though the discussion in the
421 previous paragraph likely rules out this possibility. Very recent introgression is also an unlikely
422 explanation, as our power analysis shows that the timing of introgression does not have an effect
423 at low rates. As previously discussed, directional selection on introgressed variation in the low
424 triplet could also improve the power; evaluating this possibility would be an interesting future
425 direction. Finally, we may simply have been fortunate to observe a positive result, **even with**
426 **reduced (but non-zero) power in this area of parameter space**. Distinguishing random chance
427 from other processes would also be facilitated by testing additional triplets; unfortunately, we
428 have exhausted the independent triplets possible from our data, having used six of the eight
429 available accessions with gene expression data. Very few multispecies transcriptomic datasets
430 are currently available in systems with widespread introgression, though similar tests may be

431 possible from data in the butterfly genus, *Heliconius* (Catalán et al. 2018, Catalán et al. 2019).
432 Analyzing or generating such datasets in other systems would help to confirm the generality of
433 our findings.

434 Our analysis of gene expression is consistent with the idea that introgression between wild
435 tomato species has broadly influenced variation in gene expression among species. An
436 alternative explanation is that species with more similar gene expression may be more likely to
437 introgress, possibly due to reduced negative fitness consequences from hybrid dysregulation.
438 There are again a number of pieces of evidence that argue against the latter interpretation.
439 Guerrero et al. (2016) found no evidence for an association between the magnitude of differential
440 expression between tomato introgression lines and the sterility of hybrids. While those
441 experiments had fewer generations of hybridization than wild introgressed populations—and
442 were conducted in a greenhouse—they do not indicate that general expression levels are a barrier
443 to introgression. Furthermore, here we observe a correlation between expression similarity at
444 specific genes and the tree topology inferred from their protein-coding sequences (Figure 5B).
445 This association suggests a direct causal effect of introgressed genes on their expression: *cis*-
446 regulatory differences at introgressed loci lead to a relationship between local tree topologies and
447 expression levels (cf. Scally et al. 2012). Such a relationship is highly unlikely to instead be due
448 to a barrier to introgression. The fact that we do not observe the same correlation in the "low"
449 triplet (Figure 5A) could be due either to a comparative lack of statistical power in this triplet, or
450 due to more recombination between the protein-coding regions the tree topologies were inferred
451 from and the *cis*-regulatory regions driving expression. Introgression will reduce the
452 opportunities for recombination, which could explain why the "high" triplet retains a higher
453 signal. Alternatively, it may be that *trans*-acting variation is much more common in this triplet, a
454 scenario that would not lead to an association between local gene tree topologies and local gene
455 expression. We cannot definitively distinguish among these possibilities given only the data
456 presented here. Finally, it is possible that some form of experimental or technical artefact could
457 be responsible for asymmetries in many traits, though we note that the sister species in both
458 triplets examined here always show the greatest similarity in gene expression (Supplementary
459 Tables 1 and 2). The association we observe between tree topologies and expression similarity at
460 individual genes is also inconsistent with an artefact.

461 Overall, our results demonstrate both theoretically and empirically that introgression can affect
462 patterns of quantitative trait evolution. While considerable attention and excitement has
463 justifiably been devoted to the power of introgression as an evolutionary force shaping trait
464 variation, this is a double-edged sword, as most phylogenetic comparative methods do not
465 account for gene tree discordance. Previous work has shown that discordance due solely to ILS
466 can lead to overestimates of the rate of quantitative trait evolution and to underestimates of
467 phylogenetic signal (Mendes et al. 2018). The effects of introgression in misleading our
468 inferences will be worse, as it both increases overall discordance and generates asymmetries in
469 trait sharing. Future phylogenetic comparative approaches should strive to evaluate the
470 contributions of both ILS and/or introgression on trait evolution, allowing for more accurate
471 evolutionary inferences. Doing so will pave the way for more powerful inferences about the
472 evolutionary forces that shape trait variation among species.

473

474 **Materials and Methods**

475 **Description of datasets**

476 We use ovule gene expression data that is described in Moyle et al. (2021). The dataset consists
477 of normalized quantitative expression for 14,556 genes measured in six accessions across five
478 species (two different accessions of *S. pennellii* were used in the two triplets). For each
479 accession, samples were collected on the day of flower opening for 1-4 biological replicates
480 (individual plants) grown in a common greenhouse. When applicable, we took the average
481 expression value across replicates within each accession for our analyses. Raw sequencing reads
482 for this dataset are available on the SRA under BioProject PRJNA714065. The dataset
483 containing normalized expression for each replicate, in addition to the scripts for all analyses, are
484 available from https://github.com/mhibbins/intro_quant_traits.

485 We use phylogenomic data that is described in Pease et al. (2016). The dataset consists of
486 transcriptomes from 29 accessions across 13 species, including the six accessions used in our
487 analyses. Pease et al. used MVFtools to estimate transcriptome-wide *D*-statistics for all possible
488 rooted triplets (2925 total values) across the 27 ingroup accessions. From this dataset we selected
489 the two triplets to use in our analyses. Pease et al. also inferred gene trees for each individual
490 protein-coding region (19,116 genes total) using *RAxML* (Stamatakis 2014); we used this data in
491 our gene-level analyses. Both datasets are published in the Dryad repository
492 <https://doi.org/10.5061/dryad.182dv>.

493 **Simulation of quantitative traits & power analyses**

494 We simulated the effect of introgression on quantitative trait values (as shown in Figure 2) under
495 two models: an ILS-only model and a model with ILS and introgression. For the ILS-only
496 model, we used values of 1 and 1.3 for the speciation time of A and B, and the speciation of C
497 from the ancestor of A and B, respectively (all in units of $2N$ generations). The introgression
498 condition maintained the same speciation times, with the addition of an introgression event from
499 C into B at a time of 0.5, with $\delta_2 = 0.1$. Using these parameters, we used our model to construct
500 expected variance/covariance matrices with $\sigma^2 = 1$ using a custom *R* function (script available at
501 https://github.com/mhibbins/intro_quant_traits/blob/main/scripts/bm_model_sims.R). We then
502 simulated trait values by drawing from a multivariate normal distribution using the *R* function
503 *mvrnorm* with means of 0 and the constructed matrices.

504 We performed a power analysis to assess the statistical power of Q_3 . Using the simulation
505 approach described above, we simulated 100 trait datasets under all combinations of the
506 following parameters: 5000, 10000, and 15000 for the number of genes; 0.1, 0.5, and 1 for $t_2 - t_1$;
507 0.1, 0.25, and 0.5 for $t_1 - t_m$; and 0, 0.01, 0.05, and 0.1 for the rate of introgression. We evaluated
508 significance for each dataset using a one-sample *t*-test with $H_0: Q_3 = 0$. A result was considered a
509 true positive for our analysis when $P < 0.05$ and the sign of the mean simulated Q_3 value was
510 consistent with the simulated history of introgression.

511 **Testing quantitative traits for introgression**

512 We calculated average expression values across individual replicates of each accession before
513 estimating Q_3 for each gene. To assess the significance of both our estimated Q_3 means and
514 signs, we used bootstrap-resampling. For the mean Q_3 values, we tested the null hypothesis of Q_3
515 = 0 by randomly sampling 10,000 datasets of 14,556 genes each with replacement from the
516 empirical gene expression dataset, and estimating the mean value of each. We assessed the rank i
517 of the observed Q_3 values among these resampled datasets, and a two-tailed P -value was
518 estimated using the following formula:

$$519 \quad P = 1 - 2 * |0.5 - (i/n)|$$

520 where n is the number of observations (in this case, 10,000). This formula measures the deviation
521 of the observed value from the center of the bootstrapped dataset, which has a rank of 0.5. For
522 the sign of individual genes' Q_3 values, we tested the null hypothesis that the number of negative
523 and positive signs are equal by randomly sampling 10,000 datasets of 14,556 genes each. For
524 each resampled dataset we counted the number of negative and positive Q_3 values, ranking the
525 datasets from the one with the greatest excess of negative values to the greatest excess of positive
526 values. The rank of the observed data against these resampled datasets was calculated, and two-
527 tailed P -values were evaluated using the same formula as above.

528 For the analysis of the relationship between gene-level tree topology and expression similarity,
529 we made use of gene trees inferred using *RAXML* by Pease et al. (2016). We used the Python
530 package *ete3* (Huerta-Cepas et al. 2016) to prune these gene trees down to the accessions
531 involved in our test triplets. We then obtained the overlapping set of genes for which both
532 topologies and expression data were available, and recorded the expression “topology” based on
533 the minimum pairwise distance in expression values. The counts of gene tree topology and
534 expression topology were placed into a 3x3 contingency table for each triplet, and we tested for a
535 significant association using a χ^2 test of independence.

536

537 **Acknowledgements**

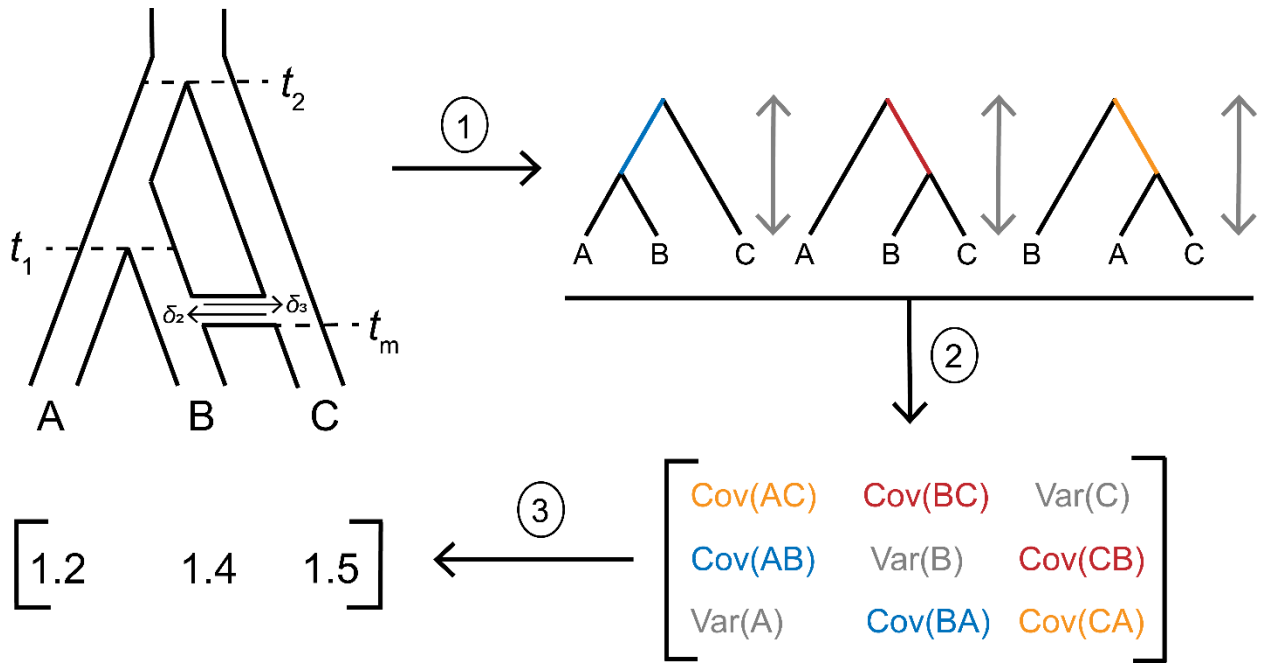
538 We thank Leonie Moyle and Matthew Gibson for sharing data, and for comments on the
539 manuscript. This work was supported by a grant from the National Science Foundation (DEB-
540 1936187).

541

542

543

544 **Figures**

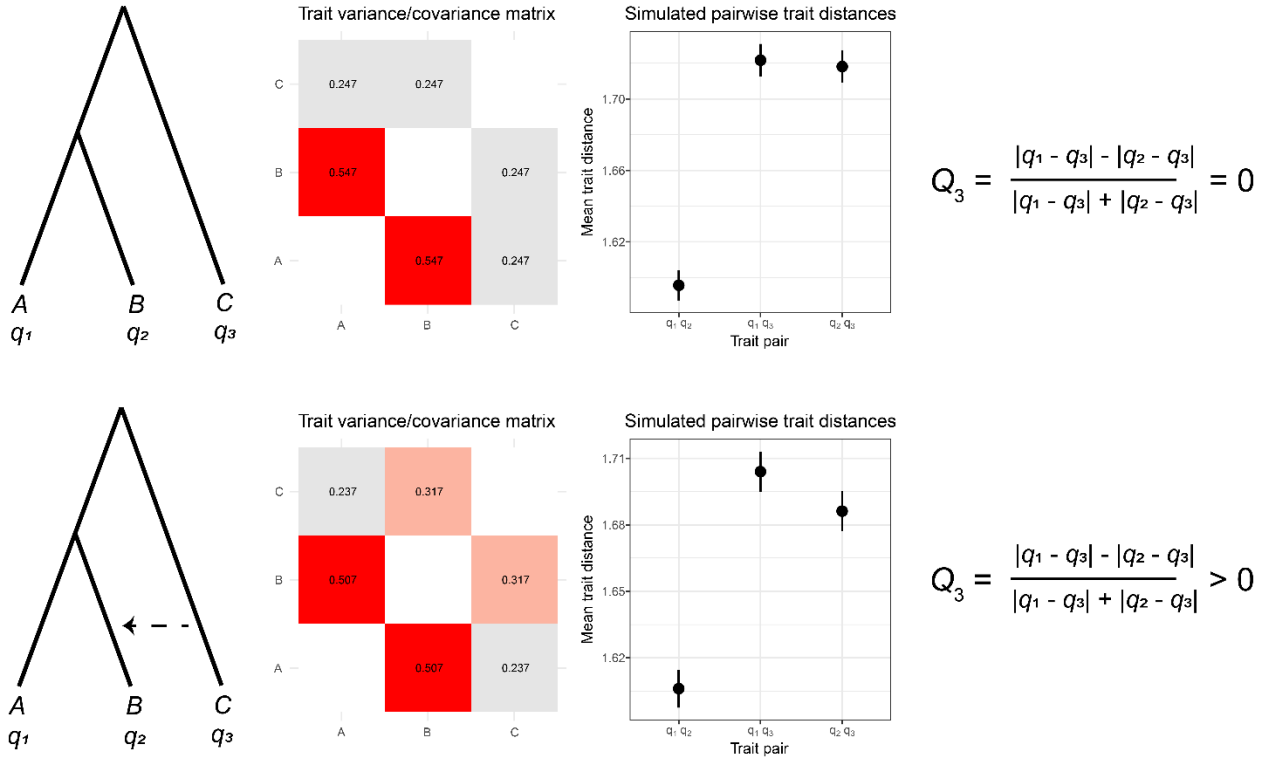


545

546 *Figure 1: Modelling quantitative trait evolution under the combined effects of ILS and*
 547 *introgression. 1) From a phylogenetic network with known parameters, the multispecies network*
 548 *coalescent model can be used to predict the expected frequency and branch lengths of each gene*
 549 *tree topology. 2) These gene trees contribute to trait covariances through their internal branches,*
 550 *and to trait variances through their total heights. The contribution of each gene tree to the overall*
 551 *quantities in T is weighted by its expected frequency. 3) Once the values of T are estimated,*
 552 *character states under Brownian motion can be simulated by drawing from a multivariate normal*
 553 *with a mean of 0 and variance of $\sigma^2 T$.*

554

555



556

557 *Figure 2: Quantifying the effect of introgression on quantitative trait variation. For ILS-only (top*
 558 *row) and ILS + introgression (bottom row) conditions, we show the expected*
 559 *variance/covariance matrix (middle-left column, variances not shown for clarity) and the average*
 560 *difference in quantitative trait values between each pair of species across 20,000 simulated traits*
 561 *(middle-right column). The expectations for the Q_3 statistic are also shown (far-right column).*

562

563

564

565

566

567

568

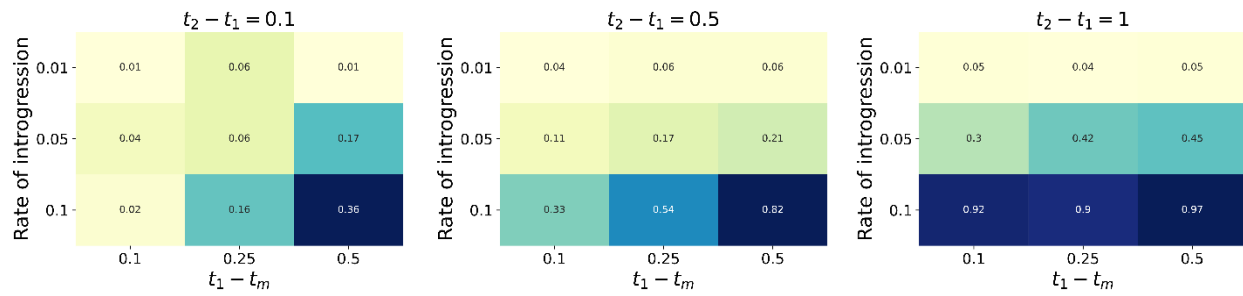
569

570

571

572

573



574

575 *Figure 3: Power analysis of the ability of Q_3 to detect a signature of introgression from 15,000*
 576 *simulated genes ($\sigma^2 = 1$). Each cell reports the proportion of 100 simulated datasets where Q_3*
 577 *was significantly different from 0 in the direction expected from the simulated history of*
 578 *introgression. Within each matrix, the x-axis is the time of introgression relative to speciation*
 579 *(larger values mean relatively more recent introgression), and the y-axis is the rate of*
 580 *introgression. There is one matrix for each of three times between speciation events, which*
 581 *determine the levels of ILS (decreasing from left to right, as the times increase). The greatest*
 582 *power comes in scenarios with little ILS, high rates of introgression, and recent introgression*
 583 *events.*

584

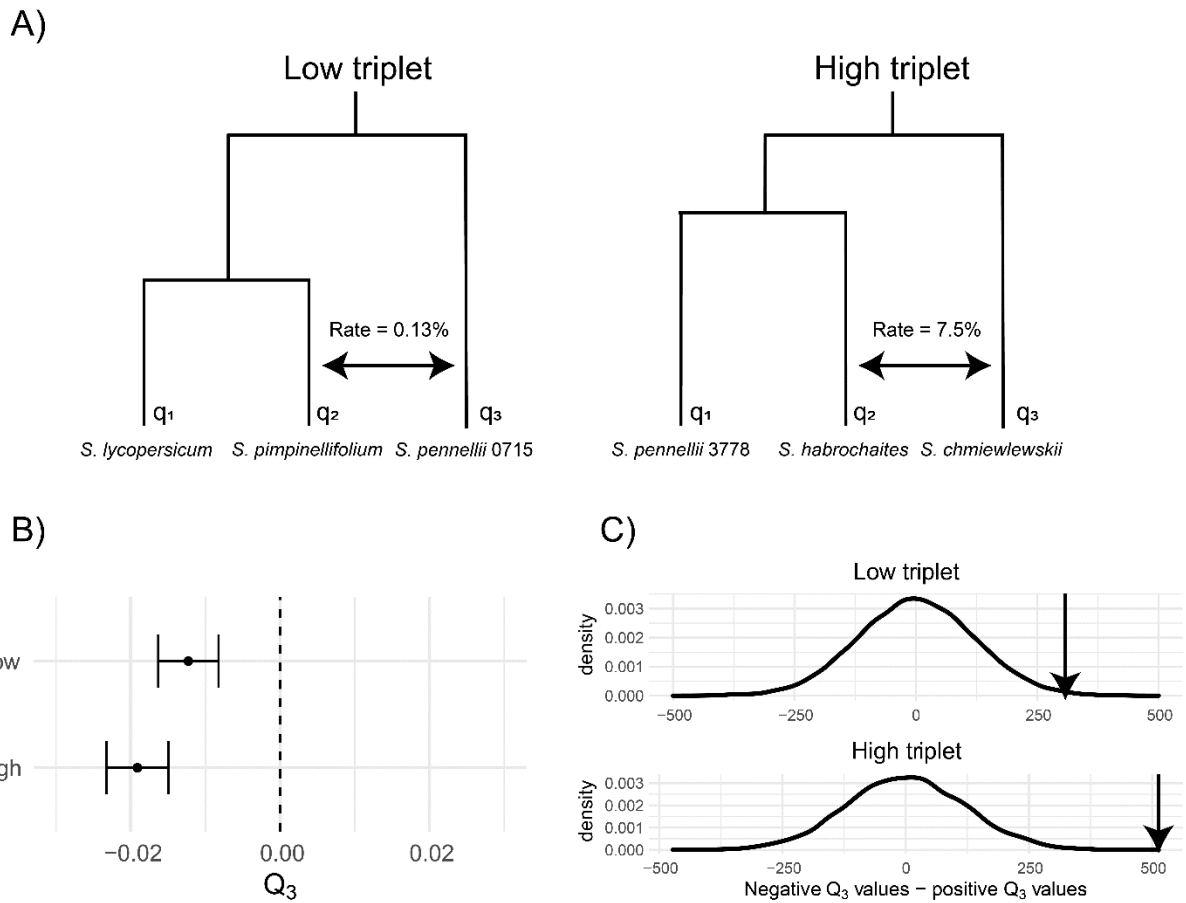
585

586

587

588

589



590

591 *Figure 4: Ovule gene expression variation in tomatoes is consistent with inferred histories of*
 592 *introgression. A) Histories of speciation and introgression for our chosen triplets in *Solanum*. B)*
 593 *Mean and standard error of Q_3 across all genes in each triplet. C) Difference in the number of*
 594 *genes with a negative vs. positive Q_3 value for both triplets. Density plots show the distribution*
 595 *of this difference across 10,000 bootstrapped datasets. Observed values for the two triplets*
 596 *relative to the bootstrap distributions are shown with arrows.*

597

598

599

600

601

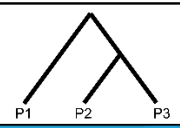
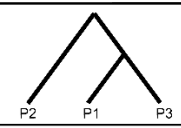
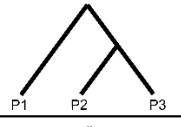
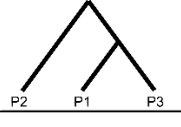
602

603

604

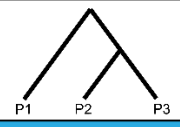
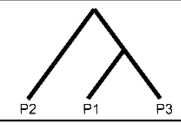
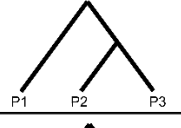
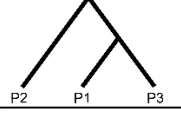
A) Low triplet

Pattern of gene expression similarity

			
Gene tree topology		O: 32 E: 34.8	O: 35 E: 32.28
		O: 22 E: 18.7	O: 18 E: 17.3

B) High triplet

Pattern of gene expression similarity

			
Gene tree topology		O: 476 E: 449.1	O: 404 E: 399.1
		O: 173 E: 187.5	O: 150 E: 166.5

605

606 *Figure 5: Relationships between coding sequence tree topology (rows) and gene expression*
 607 *similarity (columns) in the low (A) and high (B) triplets. Note that for expression similarity, we*
 608 *did not explicitly construct trees from expression data—the tree representation is simply meant*
 609 *to depict observed expression distances. Only discordant trees and expression patterns are*
 610 *shown, but χ^2 P-values (0.776 and 0.019 for panels A and B, respectively) are reported from the*
 611 *full 3x3 table (see Supplementary Tables 1 and 2 for the full tables). The cases where both the*
 612 *tree topology and pattern of expression are consistent with the inferred history of introgression*
 613 *for that triplet are highlighted in blue. Each cell reports the observed number of genes (O) in*
 614 *each category, and the number expected (E) from the χ^2 distribution.*

615

616

617

618

619

620 **References**

- 621 1. Bastide P, Solís-Lemus C, Kriebel R, William Sparks K, Ané C. Phylogenetic
622 comparative methods on phylogenetic networks with reticulations. *Systematic*
623 *Biology*. 2018;67(5):800-20.
- 624 2. Bedford T, Hartl DL. Optimization of gene expression by natural selection.
625 *Proceedings of the National Academy of Sciences of the United States of America*.
626 2009;106(4):1133-8.
- 627 3. Blomberg SP, Garland T, Jr., Ives AR. Testing for phylogenetic signal in comparative
628 data: behavioral traits are more labile. *Evolution*. 2003;57(4):717-45.
- 629 4. Brandvain Y, Kenney AM, Fligel L, Coop G, Sweigart AL. Speciation and
630 introgression between *Mimulus nasutus* and *Mimulus guttatus*. *PLoS Genetics*.
631 2014;10(6):e1004410.
- 632 5. Brawand D, Soumillon M, Necsulea A, Julien P, Csardi G, Harrigan P, et al. The
633 evolution of gene expression levels in mammalian organs. *Nature*.
634 2011;478(7369):343-8.
- 635 6. Catalán A, Briscoe AD, Hohna S. Drift and directional selection are the evolutionary
636 forces driving gene expression divergence in eye and brain tissue of *Heliconius*
637 butterflies. *Genetics*. 2019;213(2):581-94.
- 638 7. Catalán A, Macias-Muñoz A, Briscoe AD. Evolution of sex-biased gene expression
639 and dosage compensation in the eye and brain of *Heliconius* butterflies. *Molecular*
640 *Biology and Evolution*. 2018;35(9):2120-2134.
- 641 8. Chen J, Swofford R, Johnson J, Cummings BB, Rogel N, Lindblad-Toh K, et al. A
642 quantitative framework for characterizing the evolutionary history of mammalian
643 gene expression. *Genome Research*. 2019;29(1):53-63.
- 644 9. Cooper N, Thomas GH, Venditti C, Meade A, Freckleton RP. A cautionary note on
645 the use of Ornstein Uhlenbeck models in macroevolutionary studies. *Biological*
646 *Journal of the Linnean Society*. 2016;118(1):64-77.
- 647 10. Davidson RM, Gowda M, Moghe G, Lin H, Vaillancourt B, Shiu SH, et al.
648 Comparative transcriptomics of three *Poaceae* species reveals patterns of gene
649 expression evolution. *The Plant Journal*. 2012;71(3):492-502.
- 650 11. Degnan JH. Modeling hybridization under the network multispecies coalescent.
651 *Systematic Biology*. 2018;67(5):786-99.
- 652 12. Degnan JH, Rosenberg NA. Gene tree discordance, phylogenetic inference and the
653 multispecies coalescent. *Trends in Ecology and Evolution*. 2009;24(6):332-40.
- 654 13. Durand EY, Patterson N, Reich D, Slatkin M. Testing for ancient admixture between
655 closely related populations. *Molecular Biology and Evolution*. 2011;28(8):2239-52.
- 656 14. Felsenstein J. Maximum-likelihood estimation of evolutionary trees from continuous
657 characters. *American Journal of Human Genetics*. 1973;25(5):471-92.
- 658 15. Fontaine MC, Pease JB, Steele A, Waterhouse RM, Neafsey DE, Sharakhov IV, et al.
659 Extensive introgression in a malaria vector species complex revealed by
660 phylogenomics. *Science*. 2015;347(6217):1258524.

- 661 16. Gibson MJS, Torres ML, Brandvain Y, Moyle L. Introgression shapes fruit color
662 convergence in invasive Galápagos tomato. *eLife*. 2021;10:e64165.
- 663 17. Green RE, Krause J, Briggs AW, Maricic T, Stenzel U, Kircher M, et al. A draft
664 sequence of the Neandertal genome. *Science*. 2010;328(5979):710-22.
- 665 18. Guerrero RF, Posto AL, Moyle LC, Hahn MW. Genome-wide patterns of regulatory
666 divergence revealed by introgression lines. *Evolution*. 2016;70(3):696-706.
- 667 19. Hahn MW, Hibbins MS. A three-sample test for introgression. *Molecular Biology
668 and Evolution*. 2019;36(12):2878-82.
- 669 20. Hahn MW, Nakhleh L. Irrational exuberance for resolved species trees. *Evolution*.
670 2016;70(1):7-17.
- 671 21. Hamlin JAP, Hibbins MS, Moyle LC. Assessing biological factors affecting
672 postspeciation introgression. *Evolution Letters*. 2020;4(2):137-54.
- 673 22. Hansen TF. Stabilizing selection and the comparative analysis of adaptation.
674 *Evolution*. 1997;51(5):1341-51.
- 675 23. Harmon LJ, Losos JB, Jonathan Davies T, Gillespie RG, Gittleman JL, Bryan
676 Jennings W, et al. Early bursts of body size and shape evolution are rare in
677 comparative data. *Evolution*. 2010;64(8):2385-96.
- 678 24. Hibbins MS, Gibson MJ, Hahn MW. Determining the probability of hemiplasy in the
679 presence of incomplete lineage sorting and introgression. *eLife*. 2020;9:e63753
- 680 25. Hibbins MS, Hahn MW. The timing and direction of introgression under the
681 multispecies network coalescent. *Genetics*. 2019;211(3):1059-73.
- 682 26. Hill MS, Vande Zande P, Wittkopp PJ. Molecular and evolutionary processes
683 generating variation in gene expression. *Nature Reviews Genetics*. 2020;22:203-215.
- 684 27. Hime PM, Lemmon AR, Lemmon ECM, Prendini E, Brown JM, Thomson RC, et al.
685 Phylogenomics reveals ancient gene tree discordance in the amphibian tree of life.
686 *Systematic Biology*. 2021;70(1):49-66.
- 687 28. Hobolth A, Dutheil JY, Hawks J, Schierup MH, Mailund T. Incomplete lineage
688 sorting patterns among human, chimpanzee, and orangutan suggest recent orangutan
689 speciation and widespread selection. *Genome Research*. 2011;21(3):349-56.
- 690 29. Hudson RR. Testing the constant-rate neutral allele model with protein sequence data.
691 *Evolution*. 1983;37(1):203-17.
- 692 30. Huerta-Cepas J, Serra F, Bork P. ETE 3: Reconstruction, analysis, and visualization
693 of phylogenomic data. *Molecular Biology and Evolution*. 2016;33(6):1635-8.
- 694 31. Huerta-Sanchez E, Jin X, Asan, Bianba Z, Peter BM, Vinckenbosch N, et al. Altitude
695 adaptation in Tibetans caused by introgression of Denisovan-like DNA. *Nature*.
696 2014;512(7513):194-7.
- 697 32. Jones MR, Mills LS, Alves PC, Callahan CM, Alves JM, Lafferty DJR, et al.
698 Adaptive introgression underlies polymorphic seasonal camouflage in snowshoe
699 hares. *Science*. 2018;360(6395):1355-8.
- 700 33. Liu KJ, Dai J, Truong K, Song Y, Kohn MH, Nakhleh L. An HMM-based
701 comparative genomic framework for detecting introgression in eukaryotes. *PLoS
702 Computational Biology*. 2014;10(6):e1003649.

- 703 34. Mallet J, Besansky N, Hahn MW. How reticulated are species? *Bioessays*.
704 2016;38(2):140-9.
- 705 35. Martin SH, Davey JW, Salazar C, Jiggins CD. Recombination rate variation shapes
706 barriers to introgression across butterfly genomes. *PLoS Biology*.
707 2019;17(2):e2006288.
- 708 36. Mendes FK, Fuentes-Gonzalez JA, Schraiber JG, Hahn MW. A multispecies
709 coalescent model for quantitative traits. *eLife*. 2018;7:e36482
- 710 37. Meng C, Kubatko LS. Detecting hybrid speciation in the presence of incomplete
711 lineage sorting using gene tree incongruence: a model. *Theoretical Population*
712 *Biology*. 2009;75(1):35-45.
- 713 38. Moyle LC, Wu M, Gibson MJS. Reproductive proteins evolve faster than non-
714 reproductive proteins among *Solanum* species. *Frontiers in Plant Science*.
715 2021;12:635990.
- 716 39. Munch K, Nam K, Schierup MH, Mailund T. Selective sweeps across twenty millions
717 years of primate evolution. *Molecular Biology and Evolution*. 2016;33(12):3065-74.
- 718 40. Pamilo P, Nei M. Relationships between gene trees and species trees. *Molecular*
719 *Biology and Evolution*. 1988;5(5):568-83.
- 720 41. Pardo-Diaz C, Salazar C, Baxter SW, Merot C, Figueiredo-Ready W, Joron M, et al.
721 Adaptive introgression across species boundaries in *Heliconius* butterflies. *PLoS*
722 *Genetics*. 2012;8(6):e1002752.
- 723 42. Pease JB, Haak DC, Hahn MW, Moyle LC. Phylogenomics reveals three sources of
724 adaptive variation during a rapid radiation. *PLoS Biology*. 2016;14(2):e1002379.
- 725 43. Pease JB, Hahn MW. More accurate phylogenies inferred from low-recombination
726 regions in the presence of incomplete lineage sorting. *Evolution*. 2013;67(8):2376-84.
- 727 44. Pollard DA, Iyer VN, Moses AM, Eisen MB. Widespread discordance of gene trees
728 with species tree in *Drosophila*: evidence for incomplete lineage sorting. *PLoS*
729 *Genetics*. 2006;2(10):e173.
- 730 45. Reich D, Thangaraj K, Patterson N, Price AL, Singh L. Reconstructing Indian
731 population history. *Nature*. 2009;461(7263):489-94.
- 732 46. Rifkin SA, Kim J, White KP. Evolution of gene expression in the *Drosophila*
733 *melanogaster* subgroup. *Nature Genetics*. 2003;33(2):138-44.
- 734 47. Sankararaman S, Mallick S, Dannemann M, Prufer K, Kelso J, Paabo S, et al. The
735 genomic landscape of Neanderthal ancestry in present-day humans. *Nature*.
736 2014;507(7492):354-7.
- 737 48. Scally A, Dutheil JY, Hillier LW, Jordan GE, Goodhead I, Herrero J, et al. Insights
738 into hominid evolution from the gorilla genome sequence. *Nature*.
739 2012;483(7388):169-75.
- 740 49. Schumer M, Xu C, Powell DL, Durvasula A, Skov L, Holland C, et al. Natural
741 selection interacts with recombination to shape the evolution of hybrid genomes.
742 *Science*. 2018;360(6389):656-60.
- 743 50. Setter D, Mousset S, Cheng X, Nielsen R, DeGiorgio M, Hermisson J.
744 VolcanoFinder: Genomic scans for adaptive introgression. *PLoS Genetics*.
745 2020;16(6):e1008867.

- 746 51. Simpson GG. Tempo and mode in evolution. New York: Columbia University Press;
747 1944. 237 p.
- 748 52. Stamatakis A. RAxML version 8: a tool for phylogenetic analysis and post-analysis
749 of large phylogenies. *Bioinformatics*. 2014;30(9):1312-3.
- 750 53. Taylor SA, Larson EL. Insights from genomes into the evolutionary importance and
751 prevalence of hybridization in nature. *Nature Ecology and Evolution*. 2019;3(2):170-
752 7.
- 753 54. Vanderpool D, Minh BQ, Lanfear R, Hughes D, Murali S, Harris RA, et al. Primate
754 phylogenomics uncovers multiple rapid radiations and ancient interspecific
755 introgression. *PLoS Biology*. 2020;18(12):e3000954.
- 756 55. Wang Y, Cao Z, Ogilvie HA, Nakhleh L. Phylogenomic assessment of the role of
757 hybridization and introgression in trait evolution. *BioRxiv*. 2020.
- 758 56. Wen D, Yu Y, Nakhleh L. Bayesian inference of reticulate phylogenies under the
759 multispecies network coalescent. *PLoS Genetics*. 2016;12(5):e1006006.
- 760 57. White MA, Ané C, Dewey CN, Larget BR, Payseur BA. Fine-scale phylogenetic
761 discordance across the house mouse genome. *PLoS Genetics*. 2009;5(11):e1000729.
- 762 58. Whitney KD, Randell RA, Rieseberg LH. Adaptive introgression of herbivore
763 resistance traits in the weedy sunflower *Helianthus annuus*. *The American Naturalist*.
764 2006;167(6):794-807.
- 765 59. Wray GA, Hahn MW, Abouheif E, Balhoff JP, Pizer M, Rockman MV, et al. The
766 evolution of transcriptional regulation in eukaryotes. *Molecular Biology and
767 Evolution*. 2003;20(9):1377-419.
- 768 60. Wu M, Kostyun JL, Hahn MW, Moyle LC. Dissecting the basis of novel trait
769 evolution in a radiation with widespread phylogenetic discordance. *Molecular
770 Ecology*. 2018.
- 771 61. Zhang W, Dasmahapatra KK, Mallet J, Moreira GR, Kronforst MR. Genome-wide
772 introgression among distantly related *Heliconius* butterfly species. *Genome Biology*.
773 2016;17:25.